INFLUENCE OF MATERIAL SENSTITVITY TO STRESS STATE ON THE OPTIMAL DESIGN OF DEEP DRAWING TECHNOLOGICAL PROCESSES

Nikola Nikolov, Anguel Baltov*

The influence of the material sensitivity to stress state on the optimal values of three parameters of deep drawing process including die roundness radius, blank-holder pressure and revolution per minute of forming machine is presented. The different material resistance at tension and compression is considered as a reason for material sensitivity to stress state. An optimization of deep drawing process is completed under different weight influences of two criteria: minimum deformation work and minimum time for production of one piece. The two criteria are equivalent to minimum energy consumption with maximum productivity. The data for the build of objective function are obtained by simulation of deep drawing taking into account the different material resistance under one-axial tension and pressure. The methods of simulation and optimization of the process are described.

It is shown that the change of the type of stress state in the blank during forming has different influence on the hardening of material. Taking into account this effect during the design of considered deep drawing process leads to decreasing optimal values of the die roundness radius by 11–14 % and revolutions per minute of stamping machine by 10–20 %.

Key words: *deep drawing, mechanical properties, simulation, optimization*

1. Introduction

With the development of the deep drawing technological process it is useful to take into account the cases when the formed material possesses different behaviour at tension and compression. The material stress state sensitivity is taken into account in a numerical simulation procedure of deep drawing presented in this paper. Different stress-strain curves at tension and compression are used in this numerical simulation. The experimental now-a-days techniques practically eliminate the influence of the friction or specimen bulging, and the difference is due to the different microstructural resistance of the metallic material structures. The following numerical investigations are preformed in macrolevel.

In case of rolled sheet metal the hardening curves are obtained by test results of plane samples under one dimensional tension. It is well known that under conditions of one-dimensional compression the hardening curves are normally obtained by test results of samples having channels on the compressed faces. The aim of channels is to prevent the influence of internal frictional forces against resistance to deformation. This does not reflect the real conditions of stress state during the sheet metal forming. For this reason the investigations on the influence of the type of stress state on the material sensitivity represent theoretical

* N. Nikolov, A. Baltov, Institute of Mechanics, Bulgarian Academy of Sciences, Acad. G. Bontchev Street, Block 4, 1113 Sofia, Bulgaria

and practical interest [1]. The theoretical statement based on the assumptions for isotropy and continuity of deformed material gives equality of yield stresses under different stress states. But according to the experimental data for real metals and alloys true yield stresses do not coincide at different kind of stress state for one and the same strain values [2, 3, 4]. The drawing force is calculated from the stresses in the blank areas covering the die roundness.

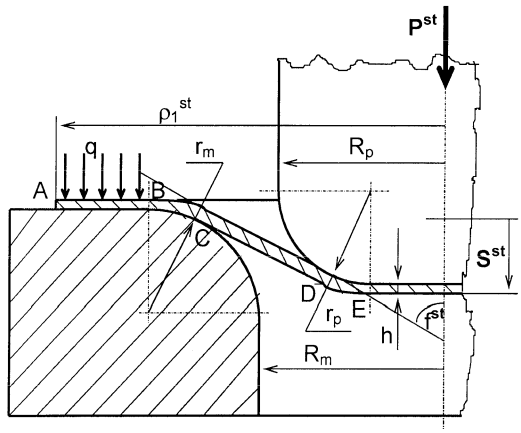

Fig. 1: Scheme of deep drawing technological process

The axis symmetric deep drawing of thin sheet metal is considered (Fig. 1). This process is characterised by changes of the kind of blank complex stress-strain state. The blank periphery is subjected to tangential compression stress state. The middle part of blank is subjected to complex stress state. The blank bottom is subjected to bi-axial tension. The influence of different material resistance causing stress state sensitivity in the blank material during blank forming may be estimated by comparison between extension and compression stress-strain diagrams [1] (Fig. 2).

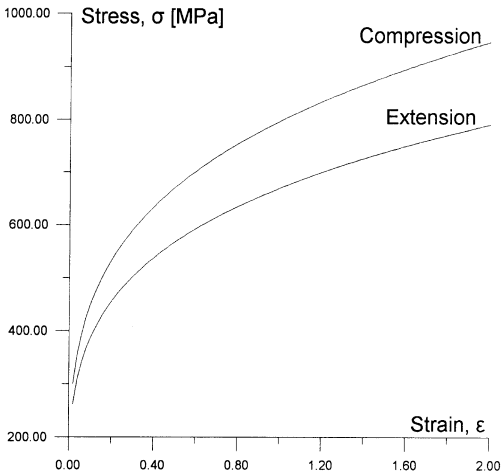

Fig.2: Stress-strain diagrams for Steel 10

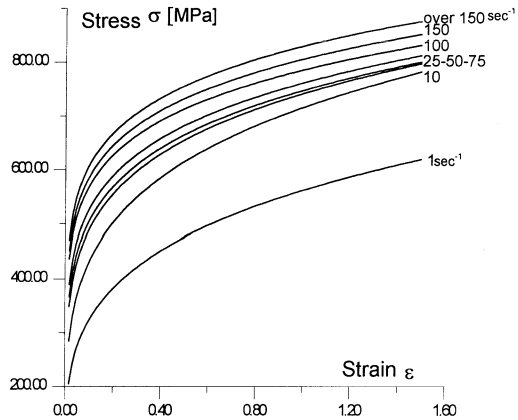

Fig.3: Change of the stress-strain diagrams for Steel 10 depending on the plastic strain rates

It is seen from reported experimental results in [2] that some materials can support higher compression stresses and lower tension ones. For example, the coefficient of different resistance given for steels, brass, aluminium and copper are 1.19, 1.15, 0.96, 1.05, respectively. A possible explanation of the effect of different material resistance can be found in the different response of metallic structures to external loading [4]. At the same time stress-strain diagram depends on the strain rate also (Fig. 3). This effect appears during quasi-static loading. A process of deep drawing can be performed by different parameter values of the forming tool design and production regimes (Fig. 1). It is possible to predict and manage the material behaviour during forming by properly designed forming stamp and corresponding forming regimes. The study of the influence of different material resistance during metal forming is a condition for achievement high limit forming ratios of blank plastic deformation without failures. For these reasons special attention must be paid to the problems of the optimization of deep drawing process as an important sheet metal forming process including variable complex stress state [5, 6, 7]. An investigation of the influence of different material resistance on the optimal values of ruling process parameters under definite optimisation criteria taken as measures of process quality represents a special interest. This will give possibilities of choice of different values for geometrical parameters of stamps from the position of taking into account more precisely the deformation process. This is the main aim of the presentation.

The present optimization is performed under two criteria : 1) minimum energy consumption for the realisation of the forming process, and 2) minimum time for the forming process. Three ruling parameters are chosen : 1) die roundness radius, 2) specific compression on the blank flange, and 3) revolutions per minute of the forming machine. The optimization assures an energetically economical production and high productivity by this formulation of the task. Comparison of the influence of different material resistance on the optimal values of ruling parameters is accomplished under above two quality criteria. By this way the material sensitivity to influence of stress state on the optimal design of forming tool and forming process is found and shown in Section 3, Figs 6 and 7.

The modelling of material behaviour is performed according to an approximate approach proposed by the authors [1]. Generally speaking, for a given level of the development of plastic strains identified by Lame index, an estimate of the different material behaviour caused by different resistance is the difference between the stress-strain diagrams obtained under compression and tension. The experiments at shearing permit to assume that the shear diagrams are close to the reduced extension diagrams.

2. Description of deep drawing process of thin rotational cylindrical pieces

2.1. Model of the process

A deep drawing of thin rotational metal pieces is considered. The technological scheme is shown in Fig. 1. The model of the process is built from : 1) the model of the blank, 2) the model of the action on the blank and 3) the model of the blank material.

2.1.1. Model of the blank

Initially, the blank represents thin circular plate, which obtains a cup form after the end of the plastic forming process. The Membrane theory of thin shells is applied during

simulation of the forming process [8, 9]. In the case of axial symmetry, the equilibrium equations are as follows [10]:

$$\frac{\partial(\varrho\, h\, \sigma_\varrho)}{\partial\alpha} - \varrho\, h\, \sigma_\theta\, \frac{\partial\varrho}{\partial\alpha} + \mu\, q\, \varrho = 0 \ , \qquad q = h\,(k_1\, \sigma_\varrho + k_2\, \sigma_\theta) \ , \tag{1}$$

where α is a local coordinate of a curvilinear coordinate system embedded in the middle surface of the sheet point having current radius $\varrho(\alpha, t)$ measured from the punch axis (Fig. 1); k_1 and k_2 are the local curvatures of the sheet; h is the current sheet thickness in the point under consideration; σ_ϱ and σ_θ are the radial and circumferential Cauchy stresses. They are functions of ϱ and the time t, $t \in [t_0;\, t_\mathrm{f}]$ (t_0 – starting moment, t_f – finishing moment of the process); μ is the friction coefficient between the surfaces of the blank and the tool; q is specific compression on the blank flange, and it is realised by blank-holder.

2.1.2. Model of the action on the blank

The sheet forming is caused by movement of cylindrical punch (Fig. 1) under action of the force P. During the forming the sheet is assumed as elastic-plastic body possessing plastic hardening according to exponential law. The forming tool elements are assumed as perfectly-rigid bodies. The punch travel S is measured by the vertical displacement of the punch front. This travel depends on the time t: $S = S(t)$, $S \in [s_0;\, s_\mathrm{f}]$, $s_0 = 0$, $s_\mathrm{f} = s(f)$ and s_f is determined from the required form of piece. It is assumed that the displacement of the punch is realised technologically by smooth and continuum path. The relation between S and t is presented by a continuous, single-valued and irreversible function. The process is controlled by the punch travel S instead of the time t. The value of the uniform specific pressure $q = q(s)$ on the blank flange (Fig. 1) is prescribed technologically. The friction between the sheet, punch, die and blank-holder is taken into account by the Coulomb law with friction coefficients μ.

2.1.3. Model of the blank material

It is assumed for the blank material [5]:

1) The blank metal (low carbon steel) is deformed plastically. There exists plastic hardening described by exponential law between the true stress and true strain. The material is plastically incompressible;
2) As a result of the different response of blank metallic structures to the variable along the blank radius complex stress state of forming process a change of blank metal behaviour can be developed. In different blank areas it leads to a different blank resistance against the forming in the case of stress state sensitive material.
3) The material is also sensitive to the strain rate, and it shows dynamical hardening (Fig. 3). In the one-dimensional case, the relation between the true stress and true strain has the following form:

$$\sigma = A^{(\pm)}\, \varepsilon^{n^{(\pm)}} \ , \tag{2}$$

where $A^{(+)}$, $n^{(+)}$, $A^{(-)}$, $n^{(-)}$ are material characteristics. They are different under tension $(+)$ and compression $(-)$, and they are functions of the strain rate $\dot{\varepsilon}$. The material characteristics are determined from one-dimensional experiments of tension and compression [2, 11].

The characteristics $A^{(+)}$ and $n^{(+)}$ are approximated analytically on the basis of one-dimensional tension experiment at different strain rates. They are properly reformed to the case of one dimensional compression [5]. In this way, the sensitivity to the stress state is taken into account on the basis of the difference between the material behaviour in tension and compression [10].

The material transversal isotropy is developed as a result of the induced anisotropy during the rolling of the metal sheet. The material is deformed as an elasto-plastic with plastic hardening and incompressibility. The Hill's law is assumed as initial yield criterion because of the initial transversal plastic anisotropy [9]. The Plastic flow theory is applied, and the constitutive equations have the following form:

$$\begin{gathered}
\mathrm{d}\varepsilon_\varrho = \mathrm{d}\lambda\,[(K_\mathrm{A}+1)\,\sigma_\varrho - K_\mathrm{A}\,\sigma_\theta]\ , \\
\mathrm{d}\varepsilon_\theta = \mathrm{d}\lambda\,[(K_\mathrm{A}+1)\,\sigma_\theta - K_\mathrm{A}\,\sigma_\varrho]\ , \\
\mathrm{d}\lambda = \frac{3\,\mathrm{d}\varepsilon_\mathrm{eq}}{2\,(K_\mathrm{A}+2)\,\sigma_\mathrm{eq}}\ , \qquad \varepsilon_\mathrm{eq} = \int_{t_0}^{t} \mathrm{d}\varepsilon_\mathrm{eq}\ , \\
\mathrm{d}\varepsilon_\mathrm{eq} = c_\mathrm{k}\sqrt{\mathrm{d}\varepsilon_\varrho^2 + b_\mathrm{k}\,\mathrm{d}\varepsilon_\varrho\,\mathrm{d}\varepsilon_\theta + \mathrm{d}\varepsilon_\theta^2}\ , \qquad \sigma_\mathrm{eq} = a_\mathrm{k}\sqrt{\sigma_\varrho^2 - b_\mathrm{k}\,\sigma_\varrho\,\sigma_\theta + \sigma_\theta^2}\ , \\
a_\mathrm{k} = \sqrt{\frac{3\,K_\mathrm{a}}{b_\mathrm{k}\,(K_\mathrm{A}+2)}}\ , \qquad b_\mathrm{k} = \frac{2\,K_\mathrm{A}}{K_\mathrm{A}+1}\ , \qquad c_\mathrm{k} = \frac{K_\mathrm{A}+1}{a_\mathrm{k}\sqrt{2\,K_\mathrm{A}+1}}
\end{gathered} \tag{3}$$

under

$$\sigma_\mathrm{eq} = a_\mathrm{k}\,\sigma\ , \qquad \varepsilon_\mathrm{eq} = \frac{1}{a_\mathrm{k}}\,\varepsilon\ , \qquad \sigma_\mathrm{eq} = B\,\varepsilon_\mathrm{eq}^n\ , \qquad B = a_\mathrm{k}^{n+1}\,A\ , \tag{4}$$

where $\mathrm{d}\varepsilon_\varrho$, $\mathrm{d}\varepsilon_\theta$ are increments of the circumferential (tangentional to the blank radius) ε_θ and the radial ε_ϱ plastic strains; K_A is the parameter of the transversal anisotropy [10]; $\mathrm{d}\lambda$ is the plastic multiplier.

The geometrical relations between the increments of linear strains and increment of radial displacement $\mathrm{d}u_\varrho = f(\varrho, t)$ are as follows:

$$\mathrm{d}\varepsilon_\varrho = \frac{\partial(\mathrm{d}u_\varrho)}{\partial\varrho}\ , \qquad \mathrm{d}\varepsilon_\theta = \frac{\mathrm{d}u_\varrho}{\varrho}\ . \tag{5}$$

The increment of linear plastic strain along the sheet thickness $\partial\varepsilon_\mathrm{z}$ is determined by the condition of the plastic incompressibility:

$$\mathrm{d}\varepsilon_\mathrm{z} = -(\mathrm{d}\varepsilon_\varrho + \mathrm{d}\varepsilon_\theta)\ . \tag{6}$$

2.2. Numerical simulation of deep drawing

The process is simulated numerically by application of an approximate discrete method (ADM) [5]. During the forming time the blank is discretesized in concentric rings with small widths (Fig. 1). The full forming time is discretesized in the steps Δt^{st} (stages) corresponding to the steps Δs^{st} of the punch travel.

Updated Lagrange's approach is applied. The displacements, strains and stresses are determined for each step Δt^{st} starting from the data calculated for the previous step Δt^{st-1}.

The infinitesimal increments of strains $\mathrm{d}\varepsilon^{st}_{\mathrm{eq}(i)}$ are substituted with finite increments $\Delta\varepsilon^{st}_{\mathrm{eq}(i)}$, $(st = 1, 2, \ldots, L)$, $(i = 1, 2, \ldots, m$, m is the number of rings). The initial non-deformed state of the blank is the initial condition for the computations. The increments are as follows:

$$\Delta\varepsilon^{st}_{\mathrm{eq}(i)} = \varepsilon^{st}_{\mathrm{eq}(i)} - \varepsilon^{st-1}_{\mathrm{eq}(i)} \ , \quad i = 1, 2, \ldots, m \ . \tag{7}$$

The displacements are determined as the difference between the radii of the considered material point at two successive steps:

$$\Delta u^{st}_{\varrho(i)} = \varrho^{st}_{(i)} - \varrho^{st-1}_{(i)} \ . \tag{8}$$

The increment of the circumferential strain (See eq. (5)) is determined by the following relation between the two stages:

$$\Delta\varepsilon^{st}_{\theta(i)} = \frac{\Delta u^{st}_{\varrho(i)}}{\varrho^{st-1}_{(i)}} \ . \tag{9}$$

The strain increments $\Delta\varepsilon^{st}_{z(i)}$, $\Delta\varepsilon^{st}_{\varrho(i)}$ and the corresponding stresses $\sigma^{st}_{\varrho(i)}$, $\sigma^{st}_{\theta(i)}$, $(i = 1, 2, \ldots, m$; $st = 1, 2, \ldots, L)$ are determined iteratively using the discrete form of the equations (1), (3), (5) and (6). The following boundary conditions are used: the first element of flange (point A, Fig. 1) must have assigned translation depending on the punch travel; the last element of the bottom (point E, Fig. 1) must have translation equal to zero corresponding to the precision of the calculations. In each stage the following verifications of the inadmissibility are done: 1) wrinkles on the flange; 2) thinning in the part between the cylindrical wall and the bottom (Fig. 1).

The strain type in each ring element is different. Depending on these the corresponding stresses-strain curves eq. (2) are taken in the computations. The Lame index for each element is calculated during every stage of the process:

$$v^{st}_{l(i)} = \frac{2\,\Delta\varepsilon^{st}_{\mathrm{II}(i)} - \Delta\varepsilon^{st}_{\mathrm{I}(i)} - \Delta\varepsilon^{st}_{\mathrm{III}(i)}}{\Delta\varepsilon^{st}_{\mathrm{I}(i)} - \Delta\varepsilon^{st}_{\mathrm{III}(i)}} \ , \quad (st = 1, 2, \ldots, L) \ , \tag{10}$$

where $\Delta\varepsilon^{st}_{J(i)}$, $(J = \mathrm{I}, \mathrm{II}, \mathrm{III}$ are the increments of principal strains, and

$$\Delta\varepsilon^{st}_{\mathrm{I}(i)} \geq \Delta\varepsilon^{st}_{\mathrm{II}(i)} \geq \Delta\varepsilon^{st}_{\mathrm{III}(i)} \ . \tag{11}$$

The material's characteristics at tension $A^{(+)}$ and $n^{(+)}$ may be used if $-1 \leq v^{st}_{\mathrm{l}(i)} \leq -0.4641$. The material's characteristics at shearing $A^{(s)}$ and $n^{(s)}$ may be used if $-0.4641 \leq v^{st}_{\mathrm{l}(i)} \leq 0.4641$. The material's characteristics at compression $A^{(-)}$ and $n^{(-)}$ may be used if $0.4641 \leq v^{st}_{\mathrm{l}(i)} \leq 1$. The above material characteristics of given material can be obtained by respective standard tests.

The deformation work used for blank forming during one stage is:

$$W^{st} = P^{st}\,\Delta s^{st} \ , \quad (st = 1, 2, \ldots, L) \ , \tag{12}$$

where Δs^{st} is the vertical axial punch displacement during the stage time Δt^{st}, and P^{st} is the axial force assumed as constant in the time interval Δt^{st}.

The drawing force P^{st} in each process stage can be calculated according to (See [5]):

$$P^{st} = 2\,\pi\,\sigma^{st}_{\varrho(i2)}\,h^{st}_{(i2)}\,\varrho^{st}_{(i2)}\,\cos(f^{st})\ , \tag{13}$$

where f^{st} is the slope of conical blank part, and $(i2)$ is the first element of this part during each stage. Since different elements (i) have the subscript $(i2)$ during the calculation stages (st) depending on the blank flange movement, the stress $\sigma^{st}_{\varrho(i2)}$ is obtained according to the equations of Plastic flow theory (3) and (4) through different relations between true stress and true strain (2) which reflect the kind of stress-strain state corresponded to the strain type in each element (10). These calculations are performed for each stage (st) and for each element (i) in the four parts of the blank during the full time $t_{\rm pr}$ of the process.

The numerical procedure described above has been applied properly in some cases to find optimal geometrical parameters of deep drawing stamps for steel [12]. It has been verified through real physical experiments [13] carried out by an experimental stamp manufactured with optimal values of the die and punch roundness radii obtained in [12] and forming of steel blanks having different diameters.

2.3. Numerical experiment

In order to show the influence of different material resistance on the parameters of deep drawing process by the differences between the experimental results and both numerical results obtained by taking into account the different material resistance to tension and compression and these ones obtained without that, a numerical simulation of deep drawing process is accomplished using the following data (see Fig. 1): blank material Steel 08, with mechanical characteristics of plastic hardening: (1) under one-dimensional tension $A^{(+)} = 530\,\text{MPa}$, $n^{(+)} = 0.24$ and (2) under one-dimensional pressure $A^{(-)} = 631\,\text{MPa}$, $n^{(-)} = 0.24$, both obtained after approximation to experimental data [2, 11]. According to the previous explanation the reduced tension diagram is assumed at shearing.

The blank diameter is $D_{\rm z} = 105\,\text{mm}$; blank thickness $h_0 = 1.5\,\text{mm}$; die radius $R_{\rm m} = 27\,\text{mm}$; punch radius $R_{\rm p} = 25\,\text{mm}$; roundness radii of die and punch $r_{\rm m} = 10\,\text{mm}$, $r_{\rm p} = 10\,\text{mm}$. Friction coefficient is $\mu = 0.1$; specific compression on the flange is $q = 2\,\text{MPa}$ and quasi-static velocity of process is assumed. The above data are taken from a real physical experiment [2]. The comparison between the numerical results obtained by the simulation (Section 2.2) and experimental ones is possible in this way. In Fig. 4, curve 1 is the experimentally obtained diagram 'Drawing force P – Punch travel S' [12].

Simulation curve 2 obtained by taking into account the change of stress-strain state in each element (see eq. (10), Section 2.2) describes the influence of different material resistance during the forming process. Simulation curve 3 describes the forming process without taking into account this difference. The taking into account the different material resistance approximates the numerical curve 2 to the experimental curve 1. The explanation of this effect is that during the computations of drawing force P^{st} (13) a more real pre-history of the deformed blank flange elements is used. The pre-history takes into account the predominated flange compression which is reflected by values of $\sigma^{st}_{\varrho(i2)}$.

The above simulation results confirm the necessity of taking into account the material sensitivity to the kind of stress state. This is a reason for taking into account the different material resistance during technological design and optimization of such processes. The deep drawing of circular thin sheets is an example for that.

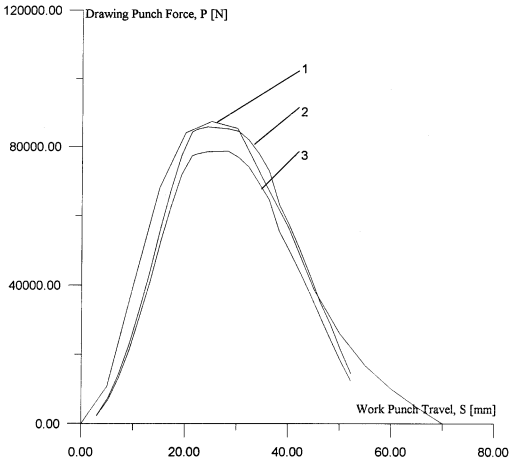

Fig.4: Diagrams 'Drawing force – Punch travel' with geometrical parameters of process $r_m = r_p = 10\,mm$, $R_p = 25\,mm$, $D_z = 105\,mm$, $h_0 = 1.5\,mm$ and material Steel 08 $\sigma = 530\varepsilon^{0.24}$; 1 – experimental diagram, [2]; 2 – simulation diagram obtained with taking into account different material resistance; 3 – simulation diagram obtained without taking into account different material resistance

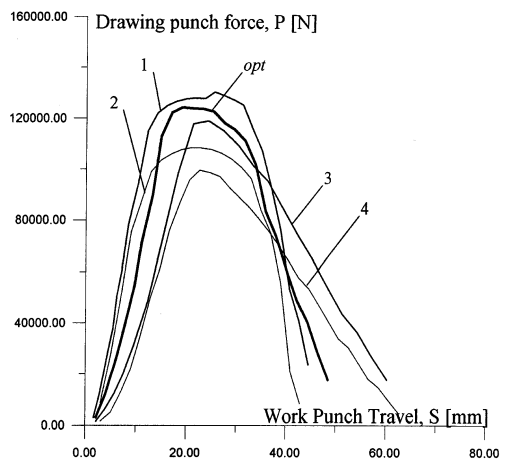

Fig.5: Diagrams 'Drawing force – Punch travel' obtained with the limit regimes in FFE-I and FFE-II and an optimal regime, (opt), (Table 2), material Steel 10 with $\sigma^+ = 670\,\varepsilon^{0.25}$; 1 – heavy duty taking into account different material resistance; 2 – heavy duty without taking into account different material resistance; 3 – light duty taking into account different material resistance; 4 – light duty without taking into account different material resistance

3. Optimization procedure for the deep drawing processes

3.1. Formulation of the optimization problem

The following optimization problem is formulated. Using the models and the simulation numerical procedure, presented briefly in Section 2, it is assumed:

(I) Optimization criteria:
  (1) Economical production;
  (2) High productivity;

(II) Ruling parameters:
  (1) Die roundness radius in the interval $4.5\,mm \leq r_m \leq 16.5\,mm$;
  (2) Blank flange compression in the interval $1.5\,MPa \leq q \leq 2.5\,MPa$;
  (3) Revolutions per minute of the forming machine in the interval $45\,min^{-1} \leq n \leq 125\,min^{-1}$, and they are corresponding to the double punch travels per minute.

These intervals are assumed on the basis of the technological experience.

The rest parameters are fixed as follows: Initial blank thickness is $h_0 = 1.5\,mm$; initial blank diameter $D_z = 105\,mm$; punch radius $R_p = 25\,mm$; punch roundness radius $r_p = 5\,mm$; full punch travel $H_p = 200\,mm$; linear punch velocity $V = 20\,m/min$. In this case the drawing coefficient is $K = 0.476$. For blank material Steel 10 the yield stress is $\sigma_S = 210\,MPa$; necking limit at tension is $\sigma_B = 340\,MPa$; initial transversal plastic anisotropy coefficient $K_A = 1.7$; friction coefficient between the surfaces of the tool and the blank is $\mu = 0.1$; work temperature of the blank $20\,°C$; plastic hardening laws under one-dimensional static tension and compression are assumed $\sigma^{(+)} = 670\,\varepsilon^{(+)^{0.25}}\,MPa$ and

$\sigma^{(-)} = 797\,\varepsilon^{(-)^{0.25}}$ MPa, respectively (σ – normal one-axial stress along the axis of sheet; ε – linear axis strain along the axis of sheet). The shear diagram is taken as reduced extension diagram according to the previous discussions.

The two optimization criteria are described by:

$$W_{\rm pr} = \sum_{st=1}^{L} P^{st}\,\Delta s^{st}\ , \qquad t_{\rm pr} = \sum_{st=1}^{L} \Delta t^{st}\ , \tag{14}$$

where the minimal work $W_{\rm pr}$ is assumed as a criterion for minimum consumption of deforming energy; L is the number of calculated stages of the process; P^{st} is the punch force, calculated by (13) and Δs^{st} is the punch displacement in the corresponding stage. The time of deforming process $t_{\rm pr}$ is assumed as a criterion for maximum process productivity.

After dimensionless of ruling parameters according to [7, 14]:

$$x_i = \frac{p_i - p_{i\,\rm cp}}{p_{i\,\rm max} - p_{i\,\rm cp}}\ , \tag{15}$$

where

$$i = 1,2,3\ ; \quad p_1 = r_{\rm m}\ , \quad p_2 = q\ , \quad p_3 = n \quad \text{and} \quad p_{i\,\rm cp} = \frac{p_{i\,\rm max} - p_{i\,\rm min}}{2} \tag{15a}$$

and dimensionless of optimization criteria completed for the first criterion, which is useful to has maximum values, according to equation:

$$y_1(p_i) = \frac{W_{\rm pr}(p_i) - W_{\rm pr\,min}}{W_{\rm pr\,max} - W_{\rm pr\,min}} \tag{16}$$

and for the second criterion, which is useful to has minimum values, according to the equation:

$$y_2(p_i) = \frac{t_{\rm pr\,max} - t_{\rm pr}(p_i)}{t_{\rm pr\,max} - t_{\rm pr\,min}} \tag{17}$$

optimization parameters and criteria are referred to as: $r_{\rm m} \equiv x_1$, $q \equiv x_2$, $n \equiv x_3$ and $y_1 \equiv W_{\rm pr}$, $y_{\rm z} \equiv t_{\rm pr}$, respectively. The new intervals of parameter change and criteria change are $(-1;+1)$ and $(0;+1)$, respectively. On the basis of these two criteria, Mean-Geometrical Objective function $Y(x_i)$ is assumed in the type:

$$Y(x_i) = \sqrt{[Y_1(x_i)]^{V_1}\,[Y_2(x_i)]^{V_2}} \tag{18}$$

where $Y_J = Y_J(x_i)$, $(J = 1,2;\ i = 1,2,3)$ are mathematical models of the optimization criteria; V_1 and V_2 are weight coefficients. They describe the importance of both the criteria during search for the optimal parameter values. The optimal parameter values appear for the maxima of function (18).

3.2. Mathematical models of the optimization criteria

Two-rate polynomial is assumed for describing of the relations $Y_J = Y_J(x_i)$:

$$Y_J = b_0 + \sum_{i=1}^{3} b_i\,x_i + \sum_{i=1}^{3}\sum_{j=i+1}^{3} b_{ij}\,x_i\,x_j + \sum_{i=1}^{3} b_{ii}\,x_i^2\ , \quad (J = 1,2)\ . \tag{19}$$

With the pointed out two levels (Section 3.1) of parameter changes, two kinds of Full Factorial Experiments (FFE) are performed according to a standard procedure [7] with influence of material resistance (FFE-I) and without that (FFE-II). The aim is to obtain the coefficients b_0, b_i, b_{ij}, b_{ii} of the polynomial (19) in these two cases.

The numerical results obtained by the design of experiments are shown in Fig. 5 for heavy duties and light duties. The results obtained with taking into account the influence of different material resistance are given with lines 1 and 3. The results obtained without the influence of different material resistance are given with lines 2 and 4. The heavy duty presented by line 1 has the parameters: minimal radius $r_{\mathrm{m}} = 4.5\,\mathrm{mm}$, and maximal values for both compression $q = 2.5\,\mathrm{MPa}$ and revolution $n = 125\,\mathrm{min}^{-1}$. The light duty presented by line 4 has the parameters: maximal radius $r_{\mathrm{m}} = 16.5\,\mathrm{mm}$, and minimal values for both the compression $q = 1.5\,\mathrm{MPa}$ and revolutions $n = 45\,\mathrm{min}^{-1}$. The possible optimal regimes of deep drawing appear in the area between these two lines. The other parameters of limit regimes are given in Table 1.

	r_{m}, mm	q, MPa	n, min^{-1}	$P_{\max}$, N	$S_{\max}$, mm	W_{pr}, J	t_{pr}, min
1	4.5	2.5	125	130293	44.54	4332	0.0497
2	4.5	1.5	45	108322	42.93	3115	0.128
3	16.5	2.5	126	118887	60.3	4051	0.0844
4	16.5	1.5	45	99500	62.6	3260	0.249
opt	9.58	1.665	114	124256	48.51	4004	0.0621

Tab.1: Values of limit regime parameters in FFE-I and FFE-II

During the computations of heavy duties 1 and 2 taking into account the different material resistance leads to an increase of the drawing force P with 15 %. This difference for the light duties is 16.5 %. Maximal difference between regimes 1 and 4 is 22.2 %. The possible optimal regimes under different influence of energy consumptions and productivity are in these limits. For example, one optimal regime *opt* calculated with values 50/50 % of pointed influence is given in Fig. 5. The optimal parameter values are also given in Table 1.

The polynomial coefficients given in Table 2 are calculated by Regression analysis [7]. The coefficients values of the models of work W_{pr} and time t_{pr} obtained with taking into account material stress state sensitivity are referred to as $W_{\mathrm{pr}}^{\mathrm{RD}}$ and $t_{\mathrm{pr}}^{\mathrm{RD}}$. The coefficients for the models of work W_{pr} and time t_{pr} obtained without taking into account this property are referred to as to W_{pr}^{-} and t_{pr}^{-}. The model adequacies and coefficient significances are checked according to the Fisher's criterion by the table of significance [6]. Drawing up conclusions about the stress state sensitivity influence is possible by analysis of the coefficients b_0, b_i, b_{ij}, b_{ii} of polynomial (19).

Next conclusions can be drawn up looking at the coefficients b_i $(i = 1, 2, 3)$ given in Table 2. The optimal die radius influence on the work $W_{\mathrm{pr}}^{\mathrm{RD}}$ calculated by taking into account the stress state sensitivity is approximately three times the die radius influence on the work W_{pr}^{-} calculated without this sensitivity. Under conditions of the FFE-I the die curvature radius r_{m} has the largest influence upon the deformation work. On the one hand higher values of the radius lead to decreasing drawing force P^{st} in (12). On the other hand, the larger radius leads to increasing punch travel S, stages L in (15) and the time t_{pr} of process. As a whole, the higher values of r_{m} lead to increasing work needed for deformation. The work increases also with increasing specific clamping q on the blank flange. The increase is not too much because the coefficient b_2 for $W_{\mathrm{pr}}^{\mathrm{RD}}$ is lower in comparison with the other

two b_1 and b_3. The influence of revolutions n of the stamping machine, which determinate the plastic strain rate (Fig. 3), comes down to increase of the work $W_{\mathrm{pr}}^{\mathrm{RD}}$. This increase follows the increase of the material's resistance against plastic deformation with increasing strain rate, but it is lower than the same increase of work $W_{\mathrm{pr}}^{\mathrm{RD}}$ for the influence of r_{m}. The reason for that is the decreasing punch travel S in eq. (15). The influence of r_{m} on the deformation work is 3.28 times or 69 % larger than this one for the plastic strain rate. The conjugate influence of r_{m} and n according to the values of b_{13} leads to decreasing work. Coefficients b_1, b_3 obtained under conditions of FFE-II show approximately one and the same influence of r_{m} and n. The deformation work increases with increasing values for r_{m} and n. The influence of n is 5.7 % larger than this one in FFE-I. The clamping q also has a larger influence compared to the previous FFE-I. There is no conjugate influence of r_{m} and n according to FFE-II. After the comparison of the coefficients from second and third columns of Table 1 the conclusion follows that the influence of the die curvature on the deformation work increases with increasing material resistance to compression. The stress state sensitivity leads to increase 2.68 times or 62 % of the influence of r_{m} on the work and decrease of the influence of revolution with 23 %. The material's plastic hardening causes the above effects. In the case of the compression (FFE-I, FFE-II and Fig. 5) follows that the hardened material (FFE-I, curves 1 and 2) has larger resistance during passing through the roundness zone.

Coeff.	For $W_{\mathrm{pr}}^{\mathrm{RD}}$	For W_{pr}^{-}	For $t_{\mathrm{pr}}^{\mathrm{RD}}$	For t_{pr}^{-}
b_0	3467.5	2831.5	0.0906	0.0905
b_1	164.3	61.2	0.0405	0.0405
b_2	3.9	5.8	0	0
b_3	50.0	64.9	−0.0374	−0.0596
b_{12}	−3.875	−4.0	0	0
b_{23}	−0.625	−7.0	−0.0199	−0.0199
b_{13}	−8.375	0	0	0
b_{11}	371.4	399.5	0.0097	0.0098
b_{22}	14.43	9.5	0.0014	0.0012
b_{33}	19.93	18.0	0.0271	0.0273

Tab.2: Coefficients of polynomial (19)

The coefficients obtained by FFE-I and FFE-II for the models (19) of both the forming process times are given in columns 4 and 5 of Table 2. The similarity of coefficients shows that the stress state sensitivity does not have important influence on the full forming process time.

3.3. Optimization tasks

The maximum of the Objective function (18) calculated under different weight coefficients V_1 and V_2 are found by the Deformable simplex optimization method of Nelder-Mead [14]. The optimal values of the roundness radius r_{m} and revolutions of machine n are shown in Fig. 6 and 7, respectively. Significant change of the optimal values of blank-holder pressure is not observed. It keeps values approximately to $q = 2\,\mathrm{MPa}$. The changes of r_{m} and n obtained without taking into account the different material resistance according to the stress state are given with solid lines. The changes of r_{m} and n obtained with taking into account different material resistance as result of stress state sensitivity are given with thin lines.

From Fig. 6, it is seen that during an optimal deep drawing design, the taking into account different material resistances at tension and compression leads to decreasing optimal size of the die roundness radius r_{m}. This, as well as the increasing drawing force with taking into account stress state sensitivity (Figs. 4 and 5), can be explained by the material hardening obtained as a result of the pass through the complex stress state of the blank flange having radius larger than $0.6\,D_{\mathrm{z}}$, where the compression stresses predominated. For this reason, the hardened material is able to support higher extension stresses caused by lower radii r_{m}. The influence of the hardening on the optimal values of r_{m} is larger under weight importance of deformation work V_1 lower than 30 %. This is shown by decrease of the optimal radius r_{m} from 7–9 mm to 6–8 mm for the up and down interval limits, respectively. The difference is 14–11 %.

The different material resistances lead to decreasing optimal values of the revolutions of machine (Fig. 7). The plastic strain rate depends on the revolutions. An explanation of this is the increase of material resistance against plastic deformation. A higher deformation force is necessary consequently. This leads to decrease of revolutions. It is seen, the increase of the influence of work V_1 over 60 % and respective decrease of the influence of time V_2 to 40 % approximate the optimal values of revolutions for both the cases. The tendency is decrease of revolutions from 100 to 50 min^{-1}. In the other interval, the influence V_1 is lower than 60 %, and the average difference between the revolutions for both the cases is 10–20 %.

This analysis evidently gives the influence of the real material stress state sensitivity on the ruling parameters after optimization.

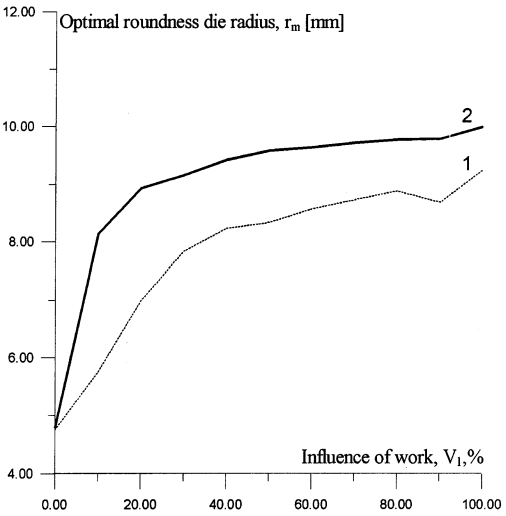

Fig.6: Optimal roundness die radii depending on the influence of deformation work: 1 – simulation diagram with taking into account different material resistance; 2 – simulation diagram without taking into account different material resistance

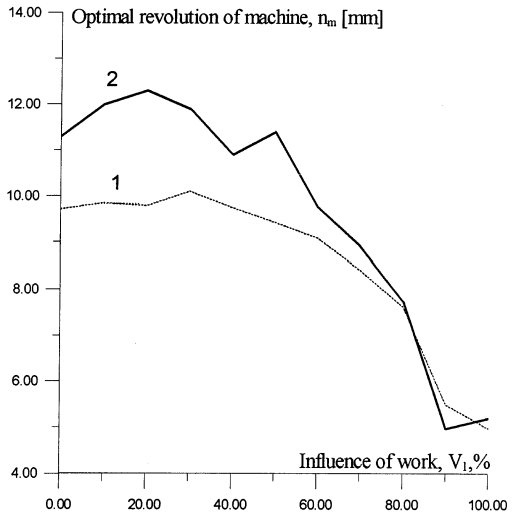

Fig.7: Optimal revolutions depending on the influence of deformation work: 1 – simulation diagram with taking into account different material resistance; 2 – simulation diagram without taking into account different material resistance

4. Conclusions

The influence of material stress state sensitivity on the optimal design of the deep drawing process has been shown (Fig. 5, 6 and 7). The numerical test examples based on the solution of the optimization problems are given. The conclusions are the following:

(a) The importance of taking into account the different material resistance at tension and compression upon the optimal values of ruling parameters is presented in the Fig. 4 and Fig. 5;

(b) The importance of weight coefficient choices upon the optimal values of ruling parameters is presented in the Fig. 6 and Fig. 7.

During computations of heavy and light duties the stress state sensitivity of the formed material (Fig. 5, Table 2) leads to an increase of drawing force P with differences 15 % and 16.5 %, respectively. This effect also leads to an increase 2.68 times or 62 % of the influence of r_{m} on the work and decrease of the influence of revolutions by 23 % (Section 3.3). The reason for that is the plastic hardening of the blank flange material, due to the pass of material along the die curvature. Taking into account the different material resistance under tension and compression during the optimal design of deep drawing processes leads to decreasing optimal values: for die roundness radius r_{m} by 11–14 % and revolutions of stamping machine by 10–20 %. This approves all presented investigations.

References

[1] Nikolov N., Baltov A.: An approximate method for damage estimation during metal forming, J. Mater. Sci. and Technology 3, (1998) 3

[2] Shofmann L.: Elements of the theory of cold stamping, 1st ed., Defence 1952, Moscow, (in Russian)

[3] Barlat F., Lian J.: Plastic behaviour and stretchability of sheet metals. Part I: A yield function for orthotropic sheet under plane stress conditions, Int. J. of Plasticity 5, (1989) 51

[4] Lubliner J.: Plasticity Theory, 2nd ed, Pearson Education 2006, Berkeley

[5] Nikolov N.: Theoretical analysis of stress-strain state during deep drawing of rotational details, Machine-Building 2–3 (2000) 15, (in Bulgarian)

[6] Daniel D., Savoie J., Jonas J. J.: Textures induced by tension and deep drawing in low carbon and extra low carbon steel sheets, Acta Metal. Mater. 41, (1993) 1907

[7] Vuchkov I., Stoyanov S.: Mathematical modelling and optimization of technological objects, 1st ed, Techniques 1996, Sofia, (in Bulgarian)

[8] Novojilov V.: Theory of thin shells, 1st ed, Machine-Building 1962, Moscow, (in Russian)

[9] Kolarov D., Baltov A., Boncheva N.: Mechanics of plastic media, 1st ed., Mir 1979, Moscow, (in Russian)

[10] Vdovin C.Iv.: Methods for calculation and design by computers of sheet metal forming processes, 1st ed, Machine-Building 1988, Moscow, (in Russian)

[11] Romanovskii V.P.: Handbook in the cold stamping, 2nd ed., Machine-Building 1979, Petersburg, (in Russian)

[12] Nikolov, N.: Optimization of geometrical parameters of deep drawing stamps, Technical ideas 3–4 (2001) 86

[13] Nikolov, N., Pashkouleva, D., Nedev, A., Kavardzhikov, V.: Experimental investigations on the deep drawing process of steel blanks, Compt. Rend. de l'Acad. Bulg. des Sci. 5 (2006) 499

[14] Stoyanov S.: Mathematical methods and algorithms for optimization, 1st ed., Technique 1990, Sofia, (in Bulgarian)

Received in editor's office: March 28, 2007
Approved for publishing: July 24, 2007